7500–7512 *Nucleic Acids Research, 2010, Vol. 38, No. 21* *Published online 29 July 2010*
doi:10.1093/nar/gkq643

The phosphatase interactor NIPP1 regulates the occupancy of the histone methyltransferase EZH2 at Polycomb targets

Nele Van Dessel[1], Lijs Beke[1], Janina Görnemann[1], Nikki Minnebo[1], Monique Beullens[1], Nobuhiro Tanuma[2], Hiroshi Shima[2], Aleyde Van Eynde[1,*] and Mathieu Bollen[1,*]

[1]Laboratory of Biosignaling and Therapeutics, Department of Molecular Cell Biology, Faculty of Medicine, KULeuven, B-3000 Leuven, Belgium and [2]Division of Cancer Chemotherapy, Miyagi Cancer Center Research Institute, Natori 981-1239, Japan

Received February 1, 2010; Revised July 6, 2010; Accepted July 7, 2010

ABSTRACT

Polycomb group (PcG) proteins are key regulators of stem-cell and cancer biology. They mainly act as repressors of differentiation and tumor-suppressor genes. One key silencing step involves the trimethylation of histone H3 on Lys27 (H3K27) by EZH2, a core component of the Polycomb Repressive Complex 2 (PRC2). The mechanism underlying the initial recruitment of mammalian PRC2 complexes is not well understood. Here, we show that NIPP1, a regulator of protein Ser/Thr phosphatase-1 (PP1), forms a complex with PP1 and PRC2 components on chromatin. The knock-down of NIPP1 or PP1 reduced the association of EZH2 with a subset of its target genes, whereas the overexpression of NIPP1 resulted in a retargeting of EZH2 from fully repressed to partially active PcG targets. However, the expression of a PP1-binding mutant of NIPP1 (NIPP1m) did not cause a redistribution of EZH2. Moreover, mapping of the chromatin binding sites with the DamID technique revealed that NIPP1 was associated with multiple PcG target genes, including the Homeobox A cluster, whereas NIPP1m showed a deficient binding at these loci. We propose that NIPP1 associates with a subset of PcG targets in a PP1-dependent manner and thereby contributes to the recruitment of the PRC2 complex.

INTRODUCTION

Polycomb group proteins are essential regulators of embryonic development and stem-cell maintenance (1–3), and their deregulation contributes to cancer (4,5). PcG proteins function as transcriptional silencers of a large set of genes, many of which are key determinants of proliferation and differentiation. PcG-mediated silencing involves two types of complexes, known as the Polycomb Repressive Complexes (PRC) 1 and 2. PRC2-type complexes initiate gene silencing through trimethylation of histone H3 on Lys27 (H3K27me3) by enhancer of zeste 2 (EZH2). Other PRC2 components, including embryonic ectoderm development (EED) and suppressor of zeste 12 homolog (SUZ12), function as activators of EZH2. Trimethylated H3K27 serves as a docking site for the initial recruitment of PRC1-type complexes, which execute gene silencing. According to one model, PRC1 complexes hamper transcriptional elongation by RNA polymerase II, possibly as a result of their ability to compact chromatin or ubiquitylate histone H2A (3).

The mechanism underlying the recruitment of PRC complexes to their targets is only partially understood (3,5). In *Drosophila*, the targeting of PRC complexes depends on the combinatorial action of multiple DNA-binding proteins, including Pleiohomeotic (Pho) and Pho-like protein, which bind at or near Polycomb Responsive Elements (PREs) on PcG target sites. Recent data suggest that mammalian PcG targets also harbor PREs (6,7), but there is also substantial evidence

*To whom correspondence should be addressed. Tel: +32 16 33 02 90; Fax: +32 16 34 59 95; Email: aleyde.vaneynde@med.kuleuven.be
Correspondence may also be addressed to Mathieu Bollen. Tel: +32 16 34 57 01; Fax: +32 16 34 59 95; Email: mathieu.bollen@med.kuleuven.be

The authors wish it to be known that, in their opinion, the first three authors should be regarded as joint First Authors.

for a role of noncoding RNAs in the recruitment of PRC complexes (2,3,5,8). The DNA-binding protein YY1, the mammalian ortholog of Pho, interacts with the PRC2 component EED and has been implicated in the recruitment of PRC2 (9). However, only a minor overlap was noted between the binding sites of YY1 and PRC2 (10), indicating that YY1 does not function as the sole PRC2 recruiter. Recently, it was shown that the DNA-binding protein JARID2 regulates PRC2 recruitment in ES cells (11,12). Collectively, these data suggest that a variety of transcription factors may be implicated in the recruitment of PcG complexes in a combinatorial and tissue-specific manner (3,5,11,12). Finally, it has also been shown that PRC2 core components interact directly with H3K27me3 (13,14), which may serve as a maintenance mechanism for the propagation of the H3K27me3 mark to unmodified nucleosomes during DNA replication.

NIPP1 (38 kDa) was initially characterized as an RNA-associated nuclear interactor of protein Ser/Thr phosphatase-1 (15,16). Later investigations identified additional direct NIPP1 ligands, including the PRC2 core components EZH2 and EED, and revealed that NIPP1 functions as a PRC2-dependent transcriptional repressor in reporter assays (17,18). In addition, NIPP1 was found to be enriched at PcG targets and a deficiency of NIPP1 in blastocysts or cultured cells was associated with a reduced global trimethylation of H3K27 and a derepression of an important subset of PcG targets (19), indicating that NIPP1 is essential for PcG-mediated repression *in vivo*. In further agreement with this view, mouse embryos lacking NIPP1 die at around the gastrulation stage (20), a phenotype that is similar to that associated with the loss of the PRC2 core components EZH2, EED or SUZ12 (2).

Since NIPP1 interacts directly with both nucleic acids and PRC2 components, it emerged as an attractive candidate regulator of PRC2 binding to chromatin. Consistent with this notion, we show here that the loss of NIPP1 results in a reduced occupancy of EZH2 at a subset of PcG targets, whereas the overexpression of NIPP1 causes, in a PP1-dependent manner, a redistribution of EZH2 between its target genes. We also demonstrate that NIPP1-associated PP1 is not involved in the assembly of the PRC2 complex but is required for its translocation to a subset of PcG targets. Our results provide novel insights into the regulation of the chromatin recruitment of PRC2-type complexes and demonstrate links between PcG-mediated gene silencing and PP1 signaling.

MATERIALS AND METHODS

Antibodies

For chromatin immunoprecipitation (ChIP) experiments anti-H3K27Me3 (07-449), anti-EZH2 (39103 and 39639) and rabbit anti-mouse immunoglobulins (IgG) were obtained from Upstate (Dundee, UK), Active motif (Rixensart, Belgium) and DakoCytomation (Gostrup, Denmark), respectively. For immunoblot analysis anti-Histone H3 (ab1791), anti-RbAp48 (ab488) and anti-TATA binding protein (ab51841) were obtained from Abcam (Cambridge, UK). Anti-SUZ12 (clone 3C1.2), mouse anti-EZH2 (AC-22) and mouse anti-NIPP1 (612368) were purchased from Millipore (Billerica, MA, USA), Cell Signaling Technology (Danvers, MA, USA) and BD Biosciences (San Jose, CA, USA), respectively, and anti-α-tubulin (clone B-5-1-2) and anti-Flag (M2, 200472-21) from Sigma-Aldrich (St. Louis, MO, USA). Anti-GFP (SC-8334) was purchased from Santa Cruz (Santa Cruz, California, USA). Monoclonal anti-PP1 antibodies, which recognize all isoforms of PP1, were purified on protein-A Sepharose CL-4B (GE Healthcare). The hybridoma clone producing these antibodies was a kind gift of Dr. J. Vandenheede (University of Leuven). Synthetic fragments of human NIPP1 (341-PGKKPTPSLLI-351), coupled to keyhole limpet hemocyanin, were used to generate polyclonal antibodies in rabbits and were used for immunoprecipitation. The antibodies were affinity-purified on the bovine serum albumin-coupled peptides linked to CNBr-activated Sepharose 4B. Human recombinant polyhistidine-tagged EED was used to raise antibodies in rabbits as previously described (17). Subsequently, EED antibodies were coupled to HRP by the Lightning-Link HRP conjugation kit (Innova Biosciences, Cambridge, UK).

Cell culture and knockdowns

PC-3 cells were cultured in 50% Dulbecco's modified Eagle's medium (DMEM) and 50% Ham's F12 with 10% fetal calf serum (FCS), HEK293T and HeLa cells were cultured in DMEM complemented with 10% FCS. The culture conditions of HTO cells are described in (21). Transfection with plasmid DNA was carried out with Fugene-6 Transfection Reagent (Roche Applied Science). Plasmids encoding EGFP, NIPP1-EGFP and NIPP1m-EGFP have been previously described (22). In the PP1-binding mutant (NIPP1m-EGFP) the RVxF-type PP1 binding motif was mutated (V201A/F203A).

SiRNA duplexes against human NIPP1 and scrambled control siRNAs were purchased from Invitrogen (Paisley, UK). SiRNA duplexes against human PP1α, PP1β, PP1γ and control siRNAs were obtained from Dharmacon (Chicago, IL, USA). Sequences of the siRNAs are described in the Supplementary Data. Knockdowns were performed using Lipofectamine 2000 (Invitrogen) and were analyzed after 48 h, as described in (19).

ChIP and DNA adenine methyltransferase identification

ChIP assays were performed as described in (19). DNA adenine methyltransferase identification (DamID) was essentially performed as described in (23). In brief, HeLa cells were stably transfected with constructs derived from pIND-(V5)-EcoDam (24), expressing trace amounts of Dam or C-terminal fusions with full-length wild-type NIPP1 and its PP1-binding mutant (NIPP1-(1-351)-V201A/F203A), leading to methylation of genomic DNA at sites of the fusion proteins' association with chromatin. Genomic DNA was extracted and processed

to enrich for DNA fragments methylated by EcoDam. Purified DNA was analyzed by quantitative PCR, as described for ChIP, or by microarray analysis. Sequences of primers are given as Supplementary Data. To verify the expression of the full-length Dam-fusion proteins, HEK293T cells were co-transfected with the pIND-(V5)-EcoDam-NIPP1 (WT and mutant) construct and the receptor-transcription factor encoding plasmid pVgRXR (Invitrogen). 20 h post transfection, 2 μM of ponasterone A (Invitrogen) was added and the cells were harvested 24 h later. Total cell lysates in SDS sample buffer were subjected to immunoblotting, detecting endogenous NIPP1 and Dam-fusions with antibodies against NIPP1.

Microarray analysis

Microarray handling, quality control and analysis were performed by the VIB MicroArray Facility in Belgium (www.microarrays.be) and were essentially performed as described in (19). In brief, for the genome-wide gene expression profiling, the RNA from HTO-PT, HTO-NIPP1 and HTO-NIPP1m cell lines from four different experiments were isolated, labeled with a fluorescent dye and hybridized onto Whole Human Genome Oligo microarrays from Agilent (Santa Clara, CA, USA). The data from the parent cell line were used as baseline expression for comparison with the Flag-NIPP1 and Flag-NIPP1m cell lines. All gene expression data are available at GEO under the accession number GSE19642.

For the genome-wide chromatin profiling, the DamID-DNA was labeled and hybridized to a GeneChIP ENCODE 2.0R array (Affymetrix, Santa Clara, CA, USA). The array read-out was analyzed with the MAT algorithm to detect enriched genomic regions for Dam-NIPP1 and Dam-NIPP1m binding in relation to the Dam-only control (25). Signal traces and regions of significant enrichment were visualized using the Integrated Genome Browser 512m provided by Affymetrix. All damID data are available at GEO under the accession number GSE22123.

Biochemical procedures

PC-3 cells were harvested and lysed for 30–45 min at 4°C in buffer A (50 mM Tris–HCl at pH 7.5, 0.5 mM phenylmethanesulfonyl fluoride (PMSF), 0.5 mM benzamidine, 5 μM leupeptin, 1 mM dithiothreitol, 20 mM NaF), supplemented with 0.5% Triton X-100. Centrifugation of the lysates (10 min at 1800 *g*) yielded a supernatant (S) and pellet (P). The pellets were washed twice with buffer A. For the chromatin association assay (Figure 1B), the pellet was incubated for 30 min at 10°C in a shaking incubator in the presence of buffer A, without or with 20 μM His-NIPP1. Recombinant His-NIPP1 was purified from *Escherichia coli* as described in (26).

For the immunoprecipitation assays in PC-3 cells (Figure 1A), the washed chromatin pellets were resuspended in 50 mM Tris–HCl at pH 8, supplemented with 1.5 mM $CaCl_2$ and 20 mM NaF, and treated with 30 U of micrococcal nuclease (Fermentas, GmBH, St Leon-Rot, Germany) for 30 min at 37°C. The soluble and insoluble fractions were separated by centrifugation (2 min at 664 *g*). The solubilized chromatin fraction (P) and the combined fractions of nucleoplasm and cytoplasm (S) were incubated for 2 h at 4°C with polyclonal anti-NIPP1 or anti-EZH2 antibodies and anti-mouse IgG for control. Subsequently, 30 μl of protein-A-TSK beads (1:1 suspension) were added for 1 h at 4°C. After centrifugation (30 s at 425 *g*) the pellet was washed four to six times with Tris-buffered saline (TBS), supplemented with 0.1% Triton X-100 and 0.25% NP-40, and subjected to immunoblotting.

For the immunoprecipitations in HEK293T cells (Figure 7), the micrococcal nuclease-solubilized chromatin fraction was obtained as described for the PC-3 cells. Subsequently, the solubilized chromatin fraction (P) was incubated for 2–3 h at 4°C with 25 μl of GFP-Trap beads (1:1 suspension, Chromotek,

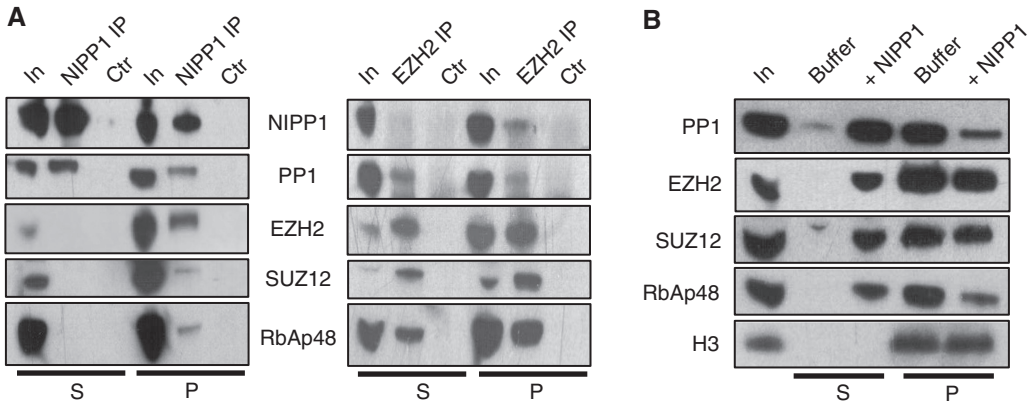

Figure 1. NIPP1 forms a complex with PP1 and PRC2 components on chromatin. (**A**) NIPP1 and EHZ2 were immunoprecipitated from the combined cytoplasmic + nucleoplasmic fractions (S) and the micrococcal nuclease-solubilized chromatin fraction (P) of PC-3 cells. Anti-mouse IgGs were used as negative control for the immunoprecipitation (Ctr). NIPP1, PP1, EZH2, SUZ12 and RBAp48 were detected by immunoblotting in the input (In, 5%) and the immunoprecipitates (IP). (**B**) The resuspended chromatin pellet of PC-3 cells was incubated for 30 min at 10°C, as such (buffer) or with 20 μM His-NIPP1. Subsequently, the insoluble fraction was resedimented. The figure shows an immunoblot of PP1, EZH2, SUZ12, RBAp48 and H3 in the input (In, 100%), supernatant (S) and pellet (P).

Planegg-Martinsried, Germany), with polyclonal EZH2 antibodies or anti-mouse IgG (Control). In the last two conditions, 30 µl of protein-A-TSK beads (1:1 suspension) were added for 1 h at 4°C. Washing conditions were identical to that used for PC-3 cells.

HTO cells (Figure 3C) were seeded and cultured for 48 h without doxycyclin. After harvesting, the cells were washed twice in PBS and lysed in buffer containing 50 mM Tris–HCl at pH 7.5, 0.3 M NaCl, 0.5 % Triton X-100, 1 mM PMSF, 1 mM benzamidine and 5 µM leupeptin for 15 min at 10°C. The lysates were clarified by centrifugation (10 min at 3800 *g*). Aliquots of cell lysates (1.7 mg protein) were incubated for 2 h at 4°C with monoclonal anti-Flag-M2 antibodies and polyclonal anti-mouse IgGs. Subsequently, 30 µl of protein-A-TSK beads (1:1 suspension) were added for 1 h at 4°C. After centrifugation (20 s at 425 *g*) the pellet was washed once with TBS supplemented with 0.1 M LiCl, twice with TBS supplemented with 0.1% NP-40, and then processed for immunoblotting. For the fractionation of HTO cells (Figure 3D), cells were lysed in buffer A, supplemented with 0.5% Triton X-100, for 45 min at 4°C and then centrifugated for 5 min at 1700 *g*. This yielded a supernatant (Sol) and the chromatin pellet (Chrom). The pellets were washed twice with buffer A, dissolved in SDS sample buffer and sonicated for 30 min at 30-s intervals.

RESULTS

Identification of a chromatin-associated complex of NIPP1, PP1 and PRC2

We have previously demonstrated that NIPP1 has distinct binding sites for PP1, EZH2 and EED, and is implicated in PRC2-mediated regulation of gene expression (17–19,22). To explore the possible role of NIPP1 and PP1 in the binding of the PRC2 complex to chromatin, we first compared their interaction in the soluble and chromatin fractions of human prostatic carcinoma (PC-3) cells. The PRC2 components EZH2, SUZ12 and RbAp48 co-immunoprecipitated with NIPP1 from a chromatin extract, but not from the combined cytoplasmic and nucleoplasmic fractions (Figure 1A). Conversely, the PRC2 components co-immunoprecipitated with EZH2 from both the soluble and chromatin fractions, but NIPP1 only co-precipitated from the chromatin extract. Finally, PP1 co-immunoprecipitated with both NIPP1 and EZH2 from the soluble and chromatin fractions. These data pointed to the existence of a chromatin-associated complex that comprises NIPP1, PP1 and PRC2 components. In further agreement with this interpretation, we found that the mere incubation of the chromatin fraction with an excess of bacterially expressed and purified NIPP1 competitively disrupted the association of EZH2, SUZ12, RbAp48 and PP1 with the chromatin pellet, but did not solubilize histone H3 (Figure 1B).

The loss of NIPP1 or PP1 reduces the targeting of EZH2

To further delineate the contribution of NIPP1 and associated PP1 to the binding of the PRC2 complex with chromatin in PC-3 cells, we examined the effect of the siRNA-mediated knockdown of either NIPP1 or PP1 (all three isoforms) on the chromatin targeting of EZH2. qRT-PCR (not shown) and immunoblot analysis (Figure 2A) showed that the transcript and protein levels of NIPP1 and PP1 could be efficiently reduced without significant effects on the concentration of EZH2. Four genes were selected to examine the effect of the knockdowns on EZH2 recruitment, namely *RPS6KC1*, *NMU* and *MYT1,* three previously established NIPP1 target genes in PC-3 cells (19), and *CDC6,* which was used as a negative control. ChIP analysis confirmed that EZH2 (Figure 2B) and H3K27me3 (Figure 2C) were enriched at the promoter region of *RPS6KC1*, *NMU* and *MYT1*. Consistent with a role for NIPP1 and PP1 in the binding of EZH2 to these target genes, the knockdown of either NIPP1 or PP1 resulted in a significantly reduced association of EZH2 with the latter three loci (Figure 2D) and a corresponding decrease in the level of H3K27me3 (Figure 2E).

The overexpression of NIPP1 redistributes EZH2

Next, we took a reverse approach and explored the effect of an overexpression of NIPP1 on the association of EZH2 with its target genes. For this purpose, we first characterized HeLa Tet-Off (HTO) cell lines that were engineered to stably express Flag-tagged wild type NIPP1 (Flag-NIPP1) or a point mutant (Flag-NIPP1m) with a disrupted PP1-docking motif (Figure 3A). The Flag fusions were only expressed in the absence of doxycyline and at levels that were up to 2-fold higher than that of endogenous NIPP1 (Figure 3B). Moreover, their expression did not affect the concentration of EZH2 and PP1. Co-immunoprecipitation analysis confirmed that Flag-NIPP1, but not Flag-NIPP1m, was associated with PP1 in HTO cell lysates (Figure 3C). However, Flag-NIPP1 and Flag-NIPP1m fractionated to a similar extent with the chromatin fraction (Figure 3D). We also performed a gene expression profiling of the HTO cell lines, using whole human genome oligo microarrays from Agilent. A paired SAM analysis identified 1365 genes with an altered expression ($P < 0.01$) between the Flag-NIPP1 and parental cell lines (Figure 3E, Supplementary Table S1). Importantly, only 185 genes were differentially expressed ($P < 0.01$) between the Flag-NIPP1m and parental cell lines (Figure 3E, Supplementary Table S2). Even more strikingly, only 5% of the genes that were affected by the expression of Flag-NIPP1 also showed a significantly different expression in the Flag-NIPP1m cells (Figure 3E). A similar small overlap was noted when the analysis was restricted to the 50 genes that were most upregulated or downregulated by the expression of Flag-NIPP1 (Figure 3F). Finally, scatter plot analysis revealed no significant correlation between the genes that were affected by the expression of Flag-NIPP1 or Flag-NIPP1m (Figure 3G). Collectively, these data demonstrate that a moderate increase in the concentration of NIPP1 affects the expression of numerous genes by a mechanism that depends on associated PP1.

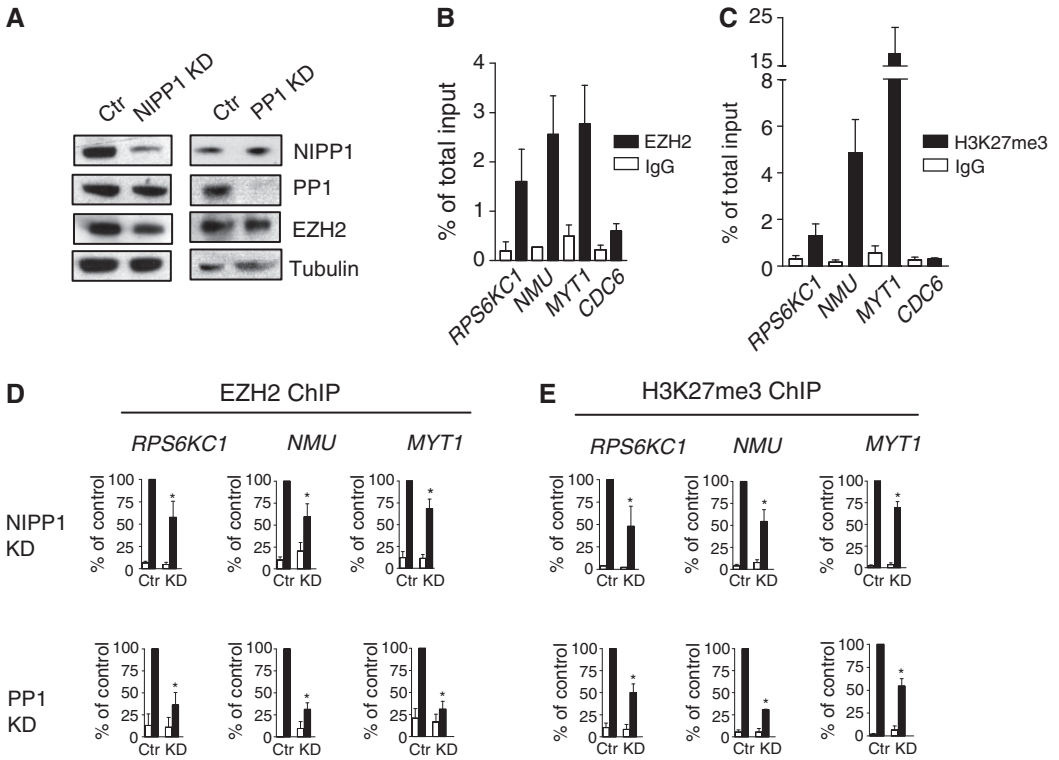

Figure 2. The downregulation of NIPP1 or PP1 is associated with a deficient binding of EZH2 to PcG target genes. (**A**) The siRNA-mediated knockdown (KD) of NIPP1 and PP1 (all three isoforms) in PC-3 cells was analyzed by immunoblotting with the indicated antibodies. Tubulin served as a loading control. (**B–E**) ChIP analysis of the indicated genes using antibodies against EZH2 (black bars in B and D) and H3K27me3 (black bars in C and E) in PC-3 cells treated with control (Ctr), NIPP1 (D and E) or PP1 (D and E) siRNAs. ChIPs with IgGs served as negative controls (white bars) and *CDC6* was used as a nontarget gene. ChIP enrichments were expressed as a percentage ± SEM ($n = 3$) of the total input signal (B and C) or as a percentage ± SEM ($n = 3$) of the data obtained with the control siRNA (D and E). $^*P < 0.05$ with the paired Student's *t*-test.

To identify PcG targets among the Flag-NIPP1 affected genes, we made use of a list of 2206 PcG target genes, as derived from a genome-wide analysis of the distribution of H3K27 trimethylation in TIG3 cells (27). Using this list, 72 of the affected genes in the Flag-NIPP1 expressing HTO cells were classified as likely PcG targets (Supplementary Table S3). However, it should be realized that the actual number of NIPP1-associated PcG target genes is probably much higher since only a minor fraction of PcG targets show an altered expression when the concentration of key PcG components is reduced (27). This has been explained by the permanent silencing of the majority of PcG targets due to secondary epigenetic modifications of the target promoters. Among these 72 putative PcG targets with altered expression, we selected six genes for further analysis, i.e. three genes that were repressed (*FOXA1, MT1F* and *C15ORF27*) and three genes that were overexpressed (*ITGB2, CCND2* and *EN1)* following the expression of Flag-NIPP1 (Figure 4A). The expression of none of these genes was affected in the Flag-NIPP1m cell line. *CDC6*, which is not a PcG target, served as a negative control in these experiments. ChIP with EZH2 and H3K27me3 antibodies confirmed that the six Flag-NIPP1 affected genes were PcG targets in HTO cells, as revealed by the binding of EZH2 (Figure 4B) and trimethylation on H3K27 (Figure 4C). Consistent with these findings, the trimethylation of H3K27 was inversely correlated with the relative transcript level (Figure 4D). Additional ChIP analyses showed that the repression of *FOXA1, MT1F* and *C15ORF27* by Flag-NIPP1 was associated with an increased EZH2 binding and trimethylation of H3K27 at the promoter region (Figure 4E). These effects were not observed after the expression of Flag-NIPP1m. A similar analysis for *ITGB2, CCND2* and *EN1* revealed that their increased transcript level after the expression of Flag-NIPP1 was associated with a decreased EZH2 binding and trimethylation of H3K27 (Figure 4F). Again, these effects were not seen after the expression of Flag-NIPP1m. In conclusion, the overexpression of NIPP1 results in an increased binding of EZH2 to a subset of PcG target genes, accounting for their increased H3K27 trimethylation and repression. In contrast, a distinct subset of PcG target genes is upregulated following the overexpression of NIPP1, and this correlates with a decreased binding of EZH2 and trimethylation of H3K27.

The association of NIPP1 with PcG target genes depends on PP1

We noted that the PcG targets (*ITGB2, CCND2* and *EN1*) that were upregulated by an overexpression of NIPP1 were initially much more repressed than the downregulated genes (*FOXA1, MT1F* and *C15ORF27*), as suggested by considerable differences in the

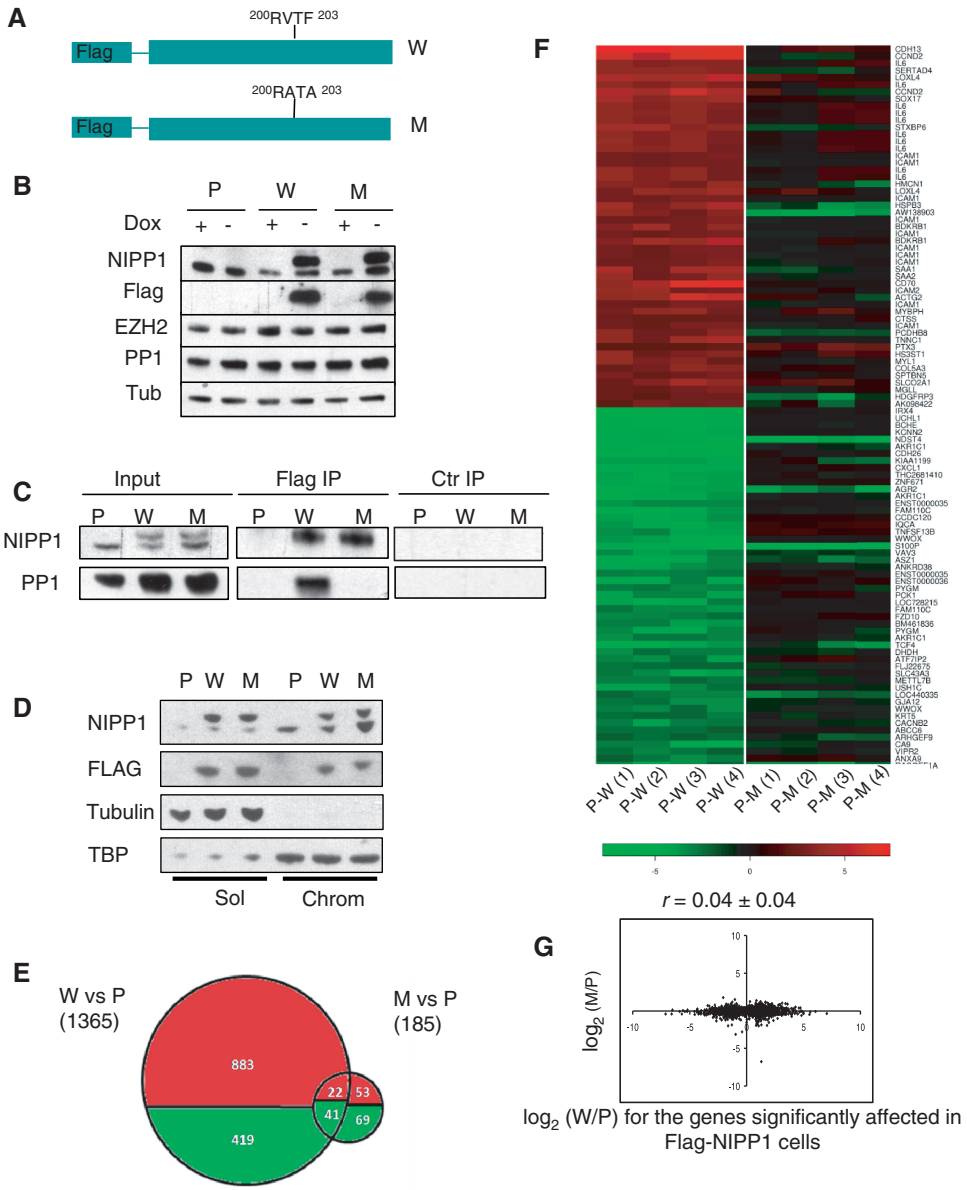

Figure 3. PP1 is required for transcriptional regulation by NIPP1. (A) Scheme of Flag-tagged wild-type NIPP1 (W) and the PP1-binding mutant of NIPP1 (M). (**B**) Parental HTO cells (P) and HTO cells that expressed Flag-tagged wild-type NIPP1 (W) or a PP1-binding mutant of NIPP1 (M) were cultured in the absence (−) or presence (+) of doxycycline (Dox). The level of NIPP1, EZH2, Flag-NIPP1 and PP1 in the cell lysates was visualized by immunoblotting. Tubulin (Tub) served as a loading control. (**C**) The Flag fusions were immunoprecipitated from the HTO cell lysates with Flag antibodies (Flag IP). IgGs were used as negative control (Ctr IP). (Co)-immunoprecipitated Flag-NIPP1 and PP1 were detected by immunoblot analysis. (**D**) The HTO cells were fractionated in a soluble (Sol) and chromatin enriched fraction (Chrom), and the level of NIPP1, Flag-NIPP1, tubulin and TATA-binding protein (TBP) in both fractions was visualized by immunoblotting. (**E**) Venn diagrams showing the overlap in genes ($P < 0.01$, SAM analysis) increased (red) or decreased (green) for the indicated comparisons. (**F**) Heat map diagram depicting the 50 most upregulated (red) and downregulated (green) genes after ectopic expression of Flag-NIPP1 as compared to parent (P-W) and of Flag-NIPP1m as compared to parent (P-M), ranked according to fold changes. The columns represent four independent experiments. The numbers on the color scheme represent the fold changes ($\log_2$ ratio). (**G**) Scatter plot of the indicated $\log_2$-transformed ratios, including the data points with significantly altered expression for the ratio indicated on the *x*-axis. The Pearson's correlation coefficient (*r*) with confidence interval is indicated.

trimethylation of H3K27 (Figure 4C) and their relative expression level (Figure 4D). Actually, this correlation generally applied to the PcG target genes in the HTO cells that were affected by the expression of Flag-NIPP1 in that the upregulated genes showed, on average, a much lower basal transcript level (Supplementary Figure 1). Therefore, one explanation for the upregulation of PcG targets by overexpressed NIPP1 is that these genes cannot bind additional NIPP1, possibly because they are already saturated with NIPP1, resulting in a re-targeting of associated EZH2 by overexpressed NIPP1 to PcG genes that can still bind additional NIPP1. An alternative explanation for the upregulation of a subset of PcG targets is that overexpressed NIPP1 competitively

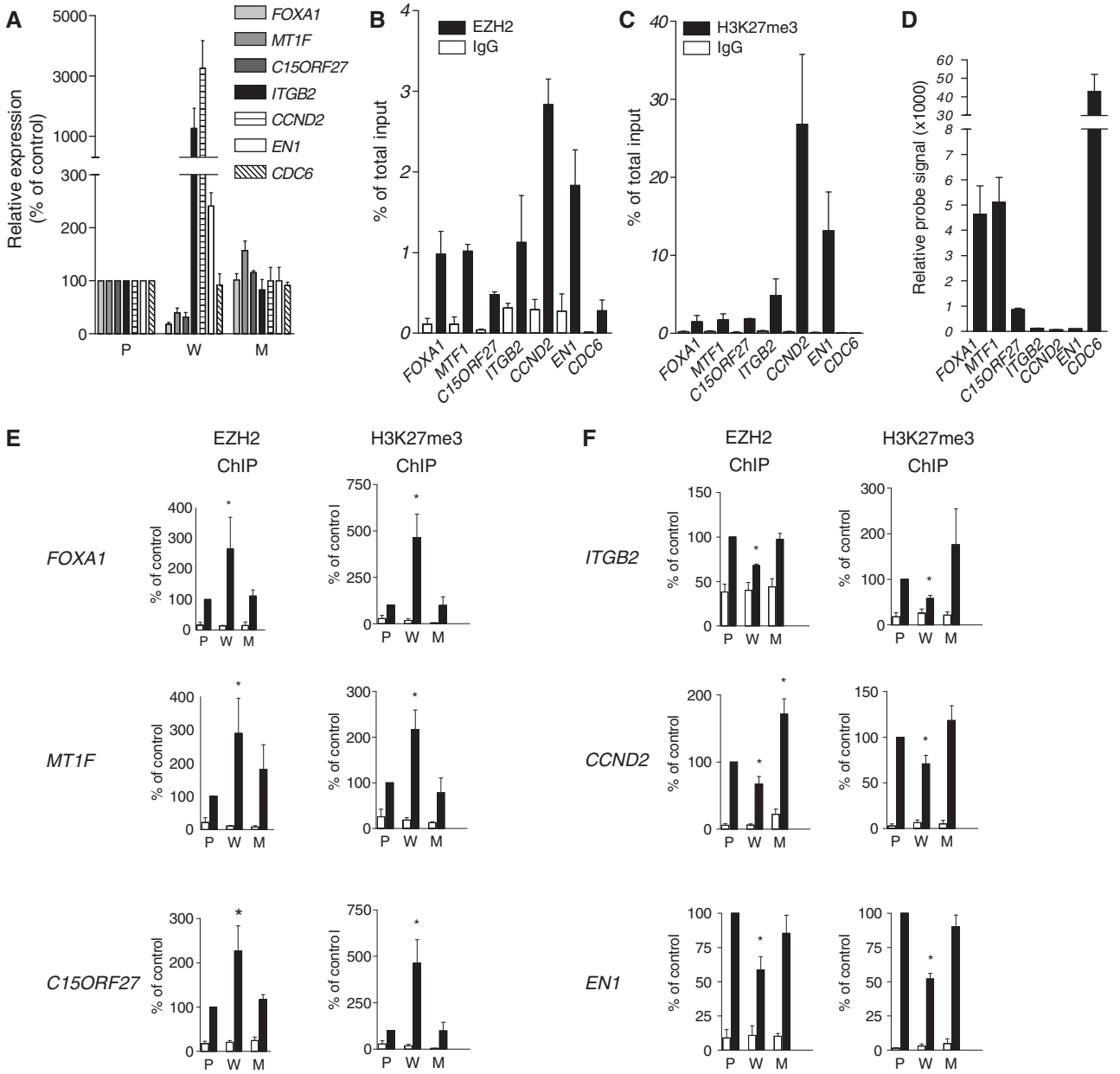

Figure 4. The overexpression of NIPP1 causes a redistribution of EZH2 among its target genes. (**A**) A bar chart of microarray data showing the relative expression levels of the indicated genes after the stable expression of Flag-NIPP1 (W) or Flag-NIPP1m (M), as a percentage ± SEM ($n = 4$) of the data obtained in the parental cell line (P). The same genes were also analyzed for the binding of EZH2 (**B**), the trimethylation of H3K27 (**C**) and their relative expression level in the parental cell line (**D**). (**E** and **F**) ChIP assays for EZH2 (left panels) and H3K27me3 (right panels) on the promoters of the indicated genes in the parental (P), Flag-NIPP1 (W) or Flag-NIPP1m (M) cells. ChIPs with rabbit anti-mouse IgGs served as negative control (white bars). ChIP enrichments were calculated as a percentage of bound/input signal (B and C) and presented as a percentage ± SEM ($n = 3$–4) of the data obtained in the parental cell line (E and F). *$P < 0.05$ with the paired Student's t-test.

disrupts the binding of PRC2 complexes to (other) chromatin recruiter proteins. The latter interpretation would imply that PcG genes that are upregulated after overexpression of NIPP1 are not direct NIPP1 targets.

Because of a discontinuity in the availability of NIPP1 antibodies of ChIP-grade, we made use of the DamID technique as an alternative tool to study the association of NIPP1 with PcG target genes *in vivo* (23,24). For that purpose, methylation-specific restriction enzymes and qPCR or microarrays were used to measure how the targeting of bacterial DNA adenine methyltransferase (Dam) that is fused to NIPP1 changes the pattern of Dam-catalyzed DNA-methylation in a GATC context (Figure 5A). HeLa cell lines stably expressing trace amounts Dam, Dam fused to NIPP1, or Dam fused to NIPP1m were generated. To rule out effects from the random integration of the transgenes, we generated and tested for each transgene two distinct polyclonal cell lines, with identical results. The expression of the transgenes in the different cell lines was verified by qRT-PCR (data not

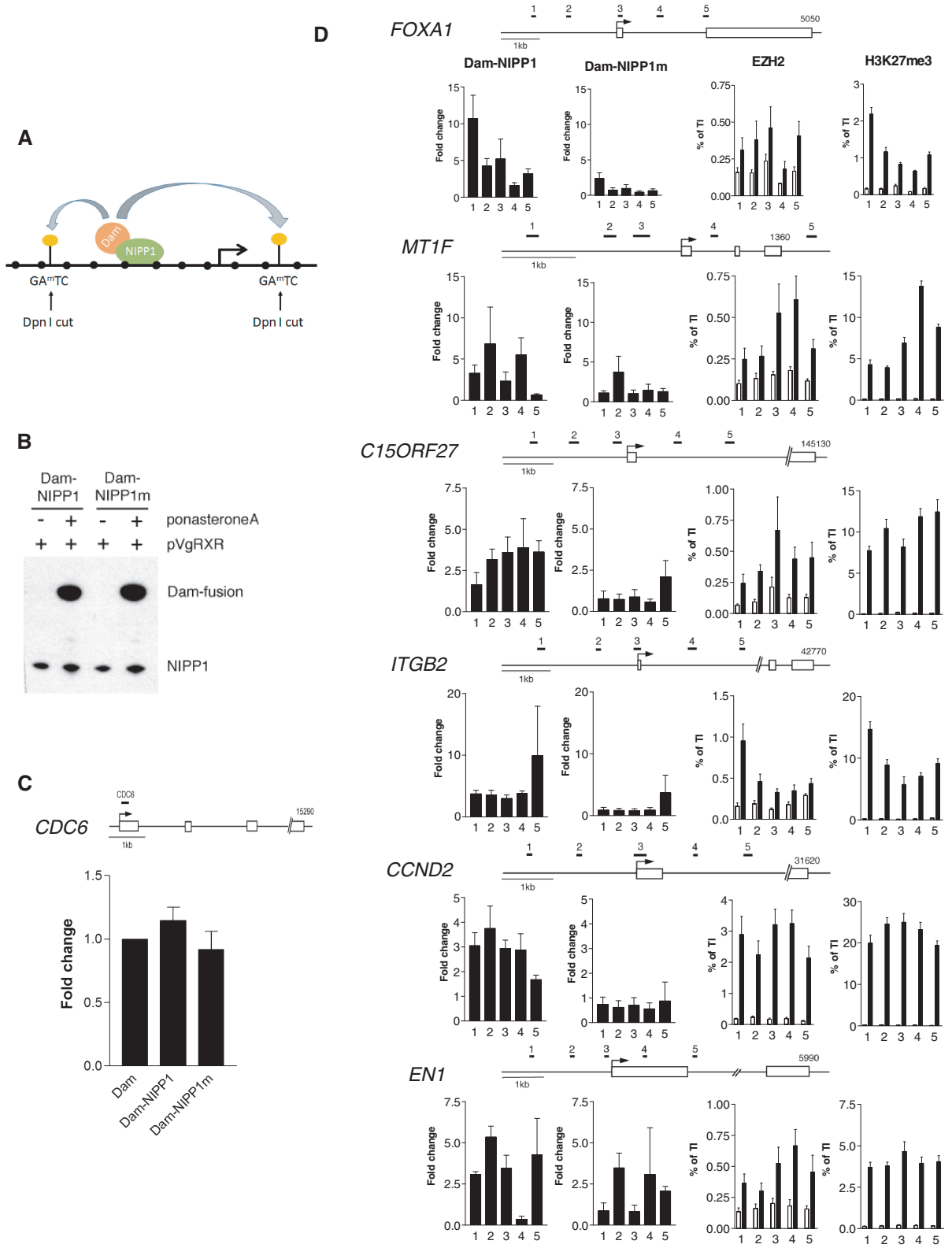

Figure 5. The association of Dam-NIPP1 with selected PcG target genes. (**A**) Scheme showing the chromatin targeting of Dam fused to NIPP1, resulting in an increased local DNA methylation. (**B**) HEK293T cells were transfected with plasmids encoding Dam-NIPP1 or Dam-NIPP1m and the activator plasmid pVgRXR, and treated with 2 μM ponasterone A. Expression of fusion proteins was verified by immunoblotting using antibodies against NIPP1. (**C** and **D**) The association of Dam, Dam-NIPP1 and Dam-NIPP1m with *CDC6* (C) and the indicated PcG genes on five positions around the transcriptional start site (D) was determined by the DamID procedure, using the same amount of total DNA for each sample. Relative abundance, as measured by qPCR, was normalized to the Dam control. ChIP assays for EZH2 and H3K27me3 on the same locations of the indicated PcG targets were performed in the Dam control cells. ChIPs with rabbit anti-mouse IgGs served as negative control (white bars) and ChIP enrichments were calculated as a percentage of bound/input signal. The positions of the PCR amplicons (numbers 1–5) on each gene are indicated on scale. Exons are indicated by white boxes and the transcriptional start site by an arrow. The data represent means ± SEM of three independent experiments.

shown). However, the very low expression level of the Dam fusions, which is important to reduce nontargeted background methylation (23), precluded a direct examination of their expression by immunoblotting. Therefore, we made use of the ecdyson-inducible promoter in the DamID vectors and verified that the used plasmids expressed similar levels of Dam-NIPP1 and Dam-NIPP1m, following their transient transfection together with the pVgRXR vector, which encodes the ecdyson receptor (Figure 5B). This expression was entirely dependent on the presence of the the ecdyson analogue Ponasterone A.

Using DamID analysis we found that, relative to Dam alone, Dam-NIPP1 and Dam-NIPP1m did not bind to the non-PcG target gene *CDC6* (Figure 5C). However, Dam-NIPP1 was associated with both subsets of the six selected PcG target genes, and this largely correlated with the binding of EZH2 and trimethylation of H3K27 at five loci around the transcriptional start site (Figure 5D). These results show that the upregulated as well as the downregulated PcG genes are direct NIPP1 targets. In further agreement with this conclusion, we found that both subsets of genes were upregulated following the knockdown of NIPP1 in the parental HTO cells (Supplementary Figure S2). Thus, a subset of PcG target genes, including *ITGB2*, *CCND2* and *EN1*, are upregulated by the knockdown (Supplementary Figure S2) as well as the overexpression of NIPP1 (Figure 4A). Intriguingly, with nearly all tested primer sets, the binding of Dam-NIPP1m to the PcG targets was strongly reduced, as compared to that of Dam-NIPP1 (Figure 5D), suggesting that the targeting of NIPP1 to PcG targets is dependent on PP1.

Mapping of NIPP1 chromatin binding sites

As an unbiased approach to study the association of NIPP1 and NIPP1m with chromatin, the DamID preparations were also analyzed by an ENCODE (ENCyclopedia Of Dna Elements) microarray. This array covers about 1% of the human genome (30 Mb, oligonucleotides of 25 bp with 7-bp tiling) and comprises coding, regulatory and intergenic regions. Independent runs from two distinct polyclonal cell lines for each condition showed numerous significant binding peaks for both Dam-NIPP1 and Dam-NIPP1m (Supplementary Table S4). Out of the 16 genes on the array that were predicted to be PcG targets based upon their trimethylation on H3K27 and Suz12 binding in TIG3 cells (27), six contained significant NIPP1 binding sites. Various Dam-NIPP1 binding sites were identified in the Homeobox (Hox) A cluster (Figure 6A), one of the best characterized PcG targets (4,27). Consistent with a role for NIPP1 in the binding of EZH2 to these genes, we found that a knockdown of NIPP1 was associated with a significantly reduced occupancy of EZH2 at five of the six analyzed Hox-A genes (Supplementary Figure S3). Further, in accordance with the qPCR data on selected PcG targets (Figure 5D), the Hox-A cluster generally also showed a reduced binding of Dam-NIPP1m (Figure 6A). This did not apply, however, to the non-PcG NIPP1 binding sites, which comprised the large majority of the Dam-NIPP1 and Dam-NIPP1m binding peaks. Indeed, some non-PcG binding sites retained Dam-NIPP1 and Dam-NIPP1m to a similar extent, while others bound Dam-NIPP1m even better than they did Dam-NIPP1 (Figure 6B), indicating that the absence of NIPP1m on PcG targets is not due to its inability to associate with chromatin. These differential NIPP1 and NIPP1m binding patterns were confirmed by qPCR (Figure 6A and B). Furthermore, we verified by ChIP analysis that the Hox-A cluster was heavily trimethylated on H3K27, unlike the regions that bound preferentially Dam-NIPP1m or both Dam-NIPP1 and Dam-NIPP1m (Figure 6C). Finally, a global analysis of the binding peaks revealed that the binding of Dam-NIPP1 and Dam-NIPP1m was relatively enriched at intronic regions, at the expense of intergenic regions (Figure 6D). In conclusion, the Dam-ID experiments revealed that both NIPP1 and NIPP1m have numerous chromatin binding sites, but the retention at a subset of PcG targets is largely restricted to NIPP1, suggesting a key contribution for PP1 in the association of NIPP1 with these loci.

PP1 is not required for the assembly of the NIPP1–PRC2 complex

The above data are suggestive for a role of PP1 in the recruitment of NIPP1 at specific PcG targets, but they do not rule out a contribution of PP1 in the assembly of the NIPP1-PRC2 complex. To address this issue, we transiently expressed EGFP, NIPP1-EGFP or NIPP1m-EGFP in HEK293T cells, isolated the EGFP complexes using 'GFP-trap' beads, and analyzed the complexes for the presence of PP1 and the PRC2 components EZH2, SUZ12, EED and RbAp48 (Figure 7A). All components, except for PP1, were similarly abundant in the immunoprecipitates of NIPP1-EGFP and NIPP1m-EGFP. Conversely, the PRC2 components were also detected equally well in EZH2 immunoprecipitates after the expression of NIPP1-EGFP or NIPP1m-EGFP (Figure 7B). Thus, PP1 does not appear to be required for the assembly of the PRC2 complex or its association with NIPP1, but is involved in the targeting or retention of the complex at a subset of PcG target sites.

DISCUSSION

We have previously demonstrated that NIPP1 has distinct binding sites for PP1 (16,22) and the PRC2 components EZH2 (18) and EED (17). Here, we show that the chromatin-associated fraction of NIPP1 and PP1, unlike its soluble pool, forms a complex with the PRC2 complex, as illustrated by reciprocal co-immunoprecipitation experiments (Figures 1A and 7A) and the ability of recombinant NIPP1 to competitively disrupt the chromatin binding of PRC2-type complexes (Figure 1B). This complex also includes the PRC2 core components SUZ12 and RbAp48, which do not interact directly with NIPP1. Moreover, a microarray- and qPCR-based DamID analysis (Figures 5 and 6) confirmed and

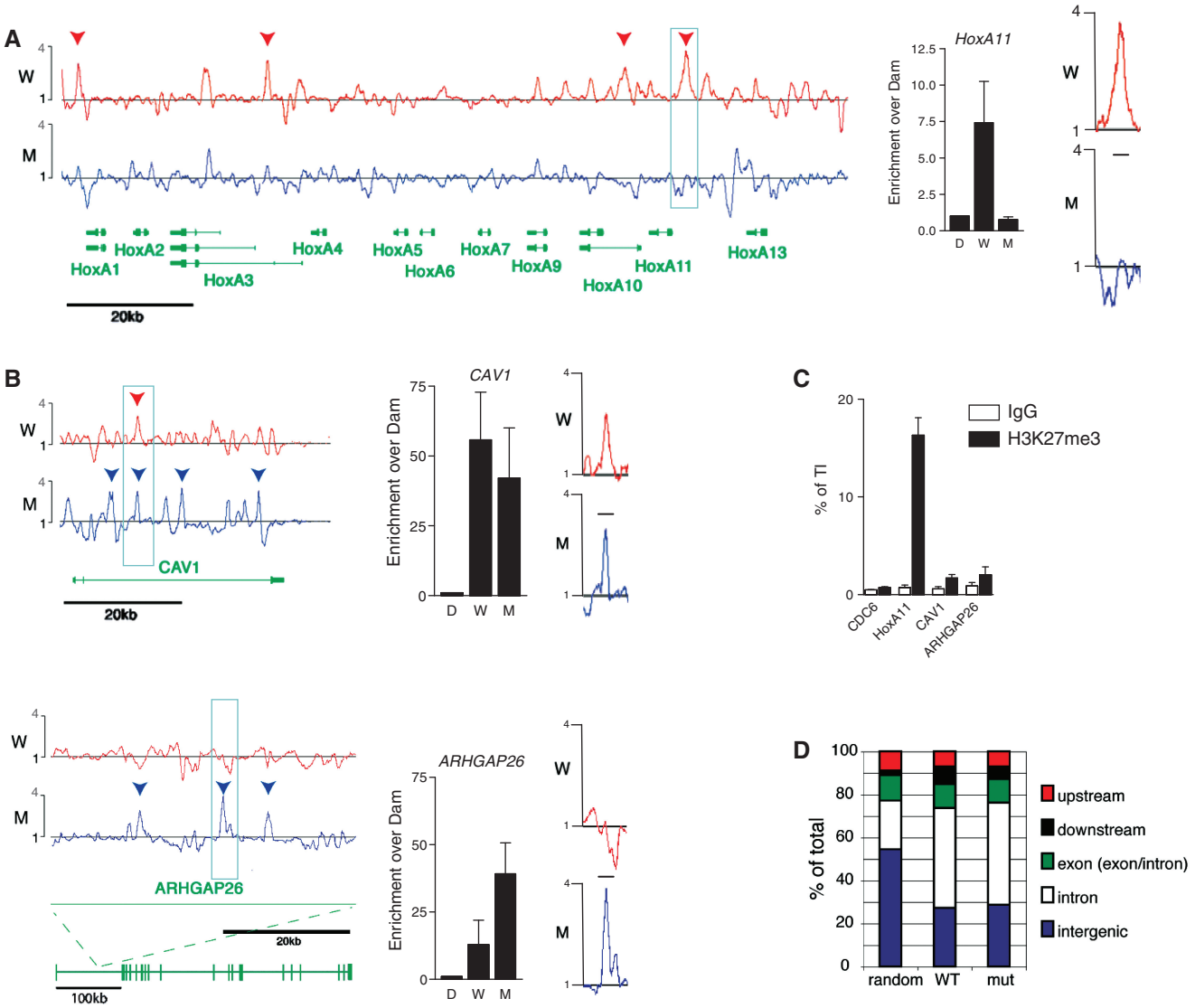

Figure 6. Genome-wide mapping of Dam-NIPP1 and Dam-NIPP1m binding sites. The binding sites were mapped by hybridisation of DNA from the DamID experiments to an ENCODE array. Two independent experiments were performed for each condition. Three representative genomic regions for differential NIPP1 binding patterns were selected. One comprises the HoxA cluster (**A**), the other two represent the *CAV1* and *ARHGAP2* genes (**B**). The red and blue lines show the distribution of Dam-NIPP1 (W) and Dam-NIPP1m (M), respectively, both in comparison to Dam (horizontal line). Arrow heads point to significant peaks as defined by the MAT algorithm, using default settings, to highlight differences and similarities between the two traces. Regions verified by qPCR (bar charts) are indicated in blue boxes and enlarged (right of the graphs). The position of the amplicon is indicated by a horizontal black line. The data were normalized to the Dam-only control and represent means ± SEM of three independent experiments. (**C**) The same genomic locations were also analyzed for trimethylation of H3K27 by qPCR analysis of ChIP experiments. The data represent means ± SEM of three independent experiments. (**D**) The significant binding sites for Dam-NIPP1 and Dam-NIPP1m were classified according to the genomic features they are representing and compared to a random distribution of features over the entire ENCODE region, according to Koch *et al.* (35). As the average NIPP1 peak is broader than most exons, some intronic sequences are also included in the 'exon' category.

extended previous ChIP data (19), showing that NIPP1 binds to PcG target sites. Among the newly identified NIPP1 targets is the Hox A cluster (Figure 6A), which belongs to the first and best characterized PcG targets (4,27). Unexpectedly, the DamID analysis also identified numerous NIPP1 chromatin-binding sites that were remote from PcG targets, indicating that NIPP1 also has chromatin-associated functions unrelated to PcG signaling. This is in accordance with previous findings showing that NIPP1 binds to RNA (26), is complexed to the splicing factors SAP155 (28) and CDC5L (29), and has a role in (alternative) pre-mRNA splicing (21,30). It indeed seems likely that Dam-NIPP1, as a component of the spliceosomes or splicing enhancer/silencing complexes, also leaves methylation marks on neighboring DNA during co-transcriptional (alternative) splicing. However, it cannot be ruled out that the transcriptional and splicing functions of NIPP1 are somehow connected. For example, the NIPP1 ligand and splicing factor SAP155 also functions as a linker between the PRC2 and PRC1 complex (31). Moreover, NIPP1 binds with high affinity to RNA (26) and noncoding RNAs have

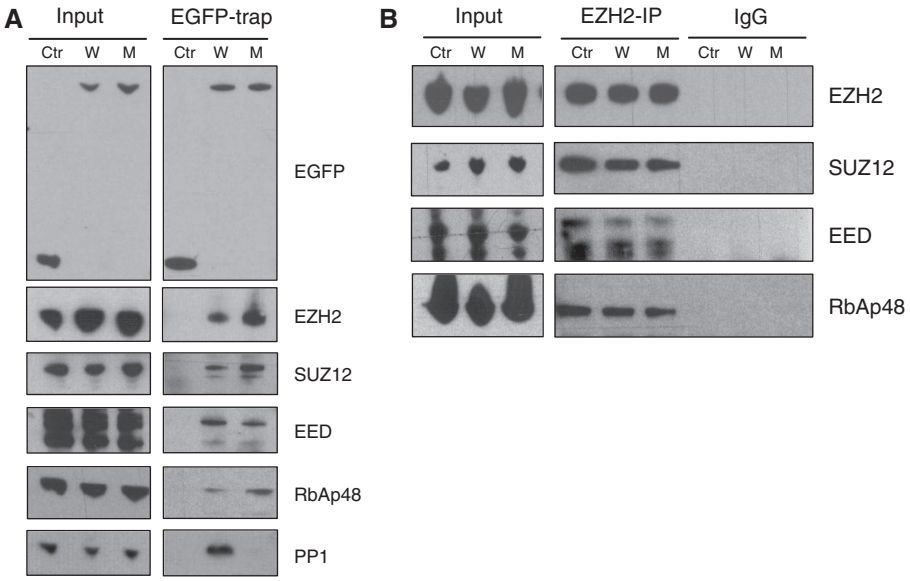

Figure 7. NIPP1-associated PP1 is not required for the NIPP1–PRC2 interaction. HEK293T cells were transfected with plasmids encoding EGFP, NIPP1-EGFP and NIPP1m-EGFP. The EGFP-fusions (**A**) and EZH2 (**B**) were immunoprecipitated from the micrococcal nuclease-solubilized chromatin fraction with the GFP-trap and anti-EZH2 antibodies, respectively. EGFP and IgG's were used as a negative control for the GFP-trap and EZH2 IP, respectively. NIPP1, EZH2, SUZ12, EED, RbAp48 and PP1 were detected by immunoblotting in the input (In, 5–10%), the GFP-trap and the immunoprecipitates (IP).

been implicated in the recruitment of PRC complexes (2,3,5,8). It will therefore be interesting to investigate whether NIPP1 regulates the targeting of PRC2-type complexes by an RNA-guided mechanism.

Our observation that NIPP1 interacts with PcG target genes as well as with the PRC2 complex makes it a prime candidate-regulator of PRC2 recruitment. Consistent with this notion, we found that the knockdown of NIPP1 resulted in a loss of EZH2 from PcG target genes and a decreased trimethylation of H3K27 (Figure 2 and Supplementary Figure S3). Conversely, the stable overexpression of NIPP1 caused a redistribution of EZH2 among PcG target genes, with corresponding changes in H3K27 trimethylation (Figure 4). Intriguingly, overexpressed NIPP1 redistributed EZH2 from maximally repressed PcG targets to genes that were still partially active (Figure 4D). Yet, both sets of PcG genes were direct NIPP1 targets, as suggested by DamID analysis (Figure 5) and their increased expression following the knockdown of NIPP1 (Supplementary Figure S2). Collectively, these data suggest that maximally repressed PcG target genes are no longer accessible to overexpressed NIPP1 or are already saturated with NIPP1. In either case, the redistribution of EZH2 can be explained by the competitive disruption of the PRC2-type complexes from fully repressed genes and their re-targeting to genes that bind the overexpressed NIPP1. At present, we do not know whether NIPP1 remains associated with PcG target genes once the PRC2 complex is recruited. It is possible that NIPP1 is only transiently associated with PcG targets and dissociates again once a chromatin structure is established that stabilizes the binding of PRC2. In this respect, it is important to note that the PRC2 complex and EED (13,14) have recently been shown to bind directly to trimethylated H3K27, which could represent a mechanism to keep PcG targets silenced once the triggers of their initial inactivation are gone. We also want to point out that the recruitment of PRC complexes in *Drosophila* is complexly regulated by multiple proteins (3). It seems likely that vertebrates also express multiple PRC recruiters or recruiter regulating proteins, as has been suggested recently (5). Additional PcG recruiter (regulating) proteins may act independently or in concert with NIPP1.

Intriguingly, the PP1-binding mutant NIPP1m still fractionated with chromatin (Figure 3D) and interacted with the PRC2 complex (Figure 7A). Yet, NIPP1m only had minor effects on transcription (Figure 3) and on the distribution and function of EZH2 (Figure 4). This is good evidence that NIPP1-associated PP1 plays a key role in NIPP1-regulated PRC2 signaling. Strikingly, we mapped numerous chromatin-binding sites for both NIPP1 and NIPP1m (Supplementary Table 4), but NIPP1m was conspicuously less associated with PcG targets (Figures 5 and 6). This suggests that NIPP1-associated PP1 is specifically needed for the targeting of NIPP1 to a subset of PcG loci. Interestingly, phosphorylation of PcG proteins is generally associated with their dissociation from chromatin (32). For example, the phosphorylation of EZH2 on Ser21 precludes its association with chromatin (33). However, the phosphorylation of this site was not different between Wt and NIPP1$^{-/-}$ blastocyst outgrowths (20). PP1-interacting proteins often act themselves as substrates or substrate targeting subunits (34). However, metabolic labeling experiments of the HTO cell lines with ^{32}P-labeled P_i did not disclose a different extent of phosphorylation of NIPP1 and NIPP1m, or their co-immunoprecipitating proteins (our unpublished data). Therefore, the

substrate(s) of NIPP1-associated PP1 that enable the binding of NIPP1 to PcG targets remain elusive and it can currently even not be ruled out entirely that the role of NIPP1-associated PP1 is structural rather than catalytic.

In conclusion, we have found that NIPP1 modulates the binding of the PRC2 complex to at least a subset of its target genes. The binding of NIPP1 to these genes depends on associated PP1, disclosing a novel interaction between PcG signaling and PP1.

SUPPLEMENTARY DATA

Supplementary Data are available at NAR Online.

ACKNOWLEDGEMENTS

Annemie Hoogmartens, Tine Jaspers, Nicole Sente, and Fabienne Withof provided expert technical assistance. We thank Rudy van Eijsden for help with the DamID analysis. N.M. is a research assistant of the FWO-Flanders.

FUNDING

Funding for open access charge: The Fund for Scientific Research-Flanders (grants KAN1.5.101.07 and G.0670.09N); Stichting tegen kanker, a Flemish Concerted Research Action (GOA10/16); Prime Minister's office (IAP/V-05).

Conflict of interest statement. None declared.

REFERENCES

1. Pietersen,A.M. and van Lohuizen,M. (2008) Stem cell regulation by polycomb repressors: postponing commitment. *Curr. Opin. Cell Biol.*, **20**, 201–207.
2. Kerppola,T.K. (2009) Polycomb group complexes - many combinations, many functions. *Trends Cell Biol.*, **19**, 692–704.
3. Simon,J.A. and Kingston,R.E. (2009) Mechanisms of polycomb gene silencing: knowns and unknowns. *Nat. Rev. Mol. Cell Biol.*, **10**, 697–708.
4. Sparmann,A. and van Lohuizen,M. (2006) Polycomb silencers control cell fate, development and cancer. *Nat. Rev. Cancer*, **6**, 846–856.
5. Bracken,A.P. and Helin,K. (2009) Polycomb group proteins: navigators of lineage pathways led astray in cancer. *Nat. Rev. Cancer*, **9**, 773–784.
6. Sing,A., Pannell,D., Karaiskakis,A., Sturgeon,K., Djabali,M., Ellis,J., Lipshitz,H.D. and Cordes,S.P. (2009) A vertebrate Polycomb response element governs segmentation of the posterior hindbrain. *Cell*, **138**, 885–897.
7. Woo,C.J., Kharchenko,P.V., Daheron,L., Park,P.J. and Kingston,R.E. (2010) A region of the human HOXD cluster that confers polycomb-group responsiveness. *Cell*, **140**, 99–110.
8. Khalil,A.M., Guttman,M., Huarte,M., Garber,M., Raj,A., Rivea,M.D., Thomas,K., Presser,A., Bernstein,B.E., van Oudenaarden,A. *et al.* (2009) Many human large intergenic noncoding RNAs associate with chromatin-modifying complexes and affect gene expression. *Proc. Natl Acad. Sci. USA*, **106**, 11667–11672.
9. Caretti,G., Di,P.M., Micales,B., Lyons,G.E. and Sartorelli,V. (2004) The Polycomb Ezh2 methyltransferase regulates muscle gene expression and skeletal muscle differentiation. *Genes Dev.*, **18**, 2627–2638.
10. Squazzo,S.L., O'Geen,H., Komashko,V.M., Krig,S.R., Jin,V.X., Jang,S.W., Margueron,R., Reinberg,D., Green,R. and Farnham,P.J. (2006) Suz12 binds to silenced regions of the genome in a cell-type-specific manner. *Genome Res.*, **16**, 890–900.
11. Pasini,D., Cloos,P.A., Walfridsson,J., Olsson,L., Bukowski,J.P., Johansen,J.V., Bak,M., Tommerup,N., Rappsilber,J. and Helin,K. (2010) JARID2 regulates binding of the Polycomb repressive complex 2 to target genes in ES cells. *Nature*, **464**, 306–310.
12. Peng,J.C., Valouev,A., Swigut,T., Zhang,J., Zhao,Y., Sidow,A. and Wysocka,J. (2009) Jarid2/Jumonji coordinates control of PRC2 enzymatic activity and target gene occupancy in pluripotent cells. *Cell*, **139**, 1290–1302.
13. Hansen,K.H., Bracken,A.P., Pasini,D., Dietrich,N., Gehani,S.S., Monrad,A., Rappsilber,J., Lerdrup,M. and Helin,K. (2008) A model for transmission of the H3K27me3 epigenetic mark. *Nat. Cell Biol.*, **10**, 1291–1300.
14. Margueron,R., Justin,N., Ohno,K., Sharpe,M.L., Son,J., Drury,W.J.III., Voigt,P., Martin,S.R., Taylor,W.R., De,M. *et al.* (2009) Role of the polycomb protein EED in the propagation of repressive histone marks. *Nature*, **461**, 762–767.
15. Jagiello,I., Beullens,M., Vulsteke,V., Wera,S., Sohlberg,B., Stalmans,W., von Gabain,A. and Bollen,M. (1997) NIPP-1, a nuclear inhibitory subunit of protein phosphatase-1, has RNA-binding properties. *J. Biol. Chem.*, **272**, 22067–22071.
16. Vulsteke,V., Beullens,M., Waelkens,E., Stalmans,W. and Bollen,M. (1997) Properties and phosphorylation sites of baculovirus-expressed nuclear inhibitor of protein phosphatase-1 (NIPP-1). *J. Biol. Chem.*, **272**, 32972–32978.
17. Jin,Q., van Eynde,A., Beullens,M., Roy,N., Thiel,G., Stalmans,W. and Bollen,M. (2003) The protein phosphatase-1 (PP1) regulator, nuclear inhibitor of PP1 (NIPP1), interacts with the polycomb group protein, embryonic ectoderm development (EED), and functions as a transcriptional repressor. *J. Biol. Chem.*, **278**, 30677–30685.
18. Roy,N., van Eynde,A., Beke,L., Nuytten,M. and Bollen,M. (2007) The transcriptional repression by NIPP1 is mediated by Polycomb group proteins. *Biochim. Biophys. Acta*, **1769**, 541–545.
19. Nuytten,M., Beke,L., van Eynde,A., Ceulemans,H., Beullens,M., Van Hummelen,P., Fuks,F. and Bollen,M. (2008) The transcriptional repressor NIPP1 is an essential player in EZH2-mediated gene silencing. *Oncogene*, **27**, 1449–1460.
20. van Eynde,A., Nuytten,M., Dewerchin,M., Schoonjans,L., Keppens,S., Beullens,M., Moons,L., Carmeliet,P., Stalmans,W. and Bollen,M. (2004) The nuclear scaffold protein NIPP1 is essential for early embryonic development and cell proliferation. *Mol. Cell Biol.*, **24**, 5863–5874.
21. Tanuma,N., Kim,S.E., Beullens,M., Tsubaki,Y., Mitsuhashi,S., Nomura,M., Kawamura,T., Isono,K., Koseki,H., Sato,M. *et al.* (2008) Nuclear inhibitor of protein phosphatase-1 (NIPP1) directs protein phosphatase-1 (PP1) to dephosphorylate the U2 small nuclear ribonucleoprotein particle (snRNP) component, spliceosome-associated protein 155 (Sap155). *J. Biol. Chem.*, **283**, 35805–35814.
22. Jagiello,I., van Eynde,A., Vulsteke,V., Beullens,M., Boudrez,A., Keppens,S., Stalmans,W. and Bollen,M. (2000) Nuclear and subnuclear targeting sequences of the protein phosphatase-1 regulator NIPP1. *J. Cell Sci.*, **113(Pt 21)**, 3761–3768.
23. Vogel,M.J., Peric-Hupkes,D. and van Steensel,B. (2007) Detection of in vivo protein-DNA interactions using DamID in mammalian cells. *Nat. Protoc.*, **2**, 1467–1478.
24. Vogel,M.J., Guelen,L., de Wit,E., Peric-Hupkes,D., Loden,M., Talhout,W., Feenstra,M., Abbas,B., Classen,A.K. and van Steensel,B. (2006) Human heterochromatin proteins form large domains containing KRAB-ZNF genes. *Genome Res.*, **16**, 1493–1504.
25. Johnson,W.E., Li,W., Meyer,C.A., Gottardo,R., Carroll,J.S., Brown,M. and Liu,X.S. (2006) Model-based analysis of tiling-arrays for ChIP-chip. *Proc. Natl Acad. Sci. USA*, **103**, 12457–12462.
26. Jin,Q., Beullens,M., Jagiello,I., van Eynde,A., Vulsteke,V., Stalmans,W. and Bollen,M. (1999) Mapping of the RNA-binding and endoribonuclease domains of NIPP1, a nuclear targeting subunit of protein phosphatase 1. *Biochem. J.*, **342(Pt 1)**, 13–19.

27. Bracken,A.P., Dietrich,N., Pasini,D., Hansen,K.H. and Helin,K. (2006) Genome-wide mapping of Polycomb target genes unravels their roles in cell fate transitions. *Genes Dev.*, **20**, 1123–1136.
28. Boudrez,A., Beullens,M., Waelkens,E., Stalmans,W. and Bollen,M. (2002) Phosphorylation-dependent interaction between the splicing factors SAP155 and NIPP1. *J. Biol. Chem.*, **277**, 31834–31841.
29. Boudrez,A., Beullens,M., Groenen,P., van Eynde,A., Vulsteke,V., Jagiello,I., Murray,M., Krainer,A.R., Stalmans,W. and Bollen,M. (2000) NIPP1-mediated interaction of protein phosphatase-1 with CDC5L, a regulator of pre-mRNA splicing and mitotic entry. *J. Biol. Chem.*, **275**, 25411–25417.
30. Novoyatleva,T., Heinrich,B., Tang,Y., Benderska,N., Butchbach,M.E., Lorson,C.L., Lorson,M.A., Ben-Dov,C., Fehlbaum,P., Bracco,L. *et al.* (2008) Protein phosphatase 1 binds to the RNA recognition motif of several splicing factors and regulates alternative pre-mRNA processing. *Hum. Mol. Genet.*, **17**, 52–70.
31. Isono,K., Mizutani-Koseki,Y., Komori,T., Schmidt-Zachmann,M.S. and Koseki,H. (2005) Mammalian polycomb-mediated repression of Hox genes requires the essential spliceosomal protein Sf3b1. *Genes Dev.*, **19**, 536–541.
32. Niessen,H.E., Demmers,J.A. and Voncken,J.W. (2009) Talking to chromatin: post-translational modulation of polycomb group function. *Epigenetics Chromatin*, **2**, 10.
33. Cha,T.L., Zhou,B.P., Xia,W., Wu,Y., Yang,C.C., Chen,C.T., Ping,B., Otte,A.P. and Hung,M.C. (2005) Akt-mediated phosphorylation of EZH2 suppresses methylation of lysine 27 in histone H3. *Science*, **310**, 306–310.
34. Bollen,M., Peti,W., Ragusa,M.J. and Beullens,M. (2010) The extended PP1 toolkit: designed to create specificity. *Trends Biochem. Sci.*, doi:10.1016/j.tibs.2010.03.002.
35. Koch,C.M., Andrews,R.M., Flicek,P., Dillon,S.C., Karaoz,U., Clelland,G.K., Wilcox,S., Beare,D.M., Fowler,J.C., Couttet,P. *et al.* (2007) The landscape of histone modifications across 1% of the human genome in five human cell lines. *Genome Res.*, **17**, 691–707.